Testing the isotropy of cosmic acceleration with the Pantheon+ and SH0ES datasets: A cosmographic analysis

Carlos A. P. Bengaly[*] and Jailson S. Alcaniz[†]
Observatório Nacional, 20921-400, Rio de Janeiro - RJ, Brazil

Cássio Pigozzo[‡]
Instituto de Física, Universidade Federal da Bahia, 40210-340, Salvador - BA, Brazil

(Received 4 March 2024; accepted 28 May 2024; published 21 June 2024)

We use a recent Pantheon + SH0ES compilation of type Ia supernova distance measurements at low-redshift, i.e., $0.01 \leq z \leq 0.10$, in order to investigate the directional dependency of the deceleration parameter (q_0) in different patches (60° size) across the sky, as a probe of the statistical isotropy of the Universe. We adopt a cosmographic approach to compute the cosmological distances, fixing H_0 and M_B to reference values provided by the collaboration. By looking at 500 different patches randomly taken across the sky, we find a maximum $\sim 3\sigma$ CL anisotropy level for q_0, whose direction points orthogonally to the cosmic microwave background (CMB) dipole axis, i.e., $(RA^{\mathrm{SN}}, DEC^{\mathrm{SN}}) = (267°, 6°)$ vs $(RA^{\mathrm{CMB}}, DEC^{\mathrm{CMB}}) = (167°, -7°)$. We assessed the statistical significance of those results, finding that such a signal is expected due to the limitations of the observational sample. These results support that there is no significant evidence for a departure from the cosmic isotropy assumption, one of the pillars of the standard cosmological model.

DOI: 10.1103/PhysRevD.109.123533

I. INTRODUCTION

One of the foundations of the current standard cosmological model, also known as Λ—cold dark matter (ΛCDM) scenario, is the assumption of the validity of the cosmological principle (*CP*) at large scales [1–5]. In other words, it states that the Universe should appear statistically homogeneous and isotropic at those scales, so that we can measure cosmological distances and ages using the Friedmann-Lemaître-Robertson-Walker (FLRW) metric. Recent analysis of redshift surveys of galaxies and quasars indicate that there is indeed a transition scale from a locally inhomogeneous Universe to a smoother, statistically homogeneous one, as described by the *CP*, at about 70–120 Mpc [6–11].

Hence, we must test the assumption of the cosmological isotropy as well in order to confirm (or rule out) the *CP* as a valid physical assumption. If ruled out, the standard model would require a profound reformulation of its basic hypotheses, including the physical origin of the mechanism behind cosmic acceleration. One possible way to test such a hypothesis involves analyzing the cosmological parameters' directional dependency, as estimated from the luminosity distance measurements of type Ia supernova (SNe). This method has been explored since the release of the earliest SN compilations, using a variety of approaches, yielding inconclusive results due to the limited sampling of objects—in terms of small number of SNe available, distance measurement uncertainties, and especially uneven sky coverage [12–33]. The latest SN compilation, namely the Pantheon + SH0ES dataset [34] (see also [35,36]), provides 1701 light curve measurements of 1550 SN objects. This corresponds to a significant improvement from previous figures of earlier SN compilations—for instance, the previous Pantheon and JLA compilations comprised 1048 and 740 SN distance measurements, respectively. However, recent analyses still yield inconclusive results regarding the validity of cosmic isotropy, depending on the sample selection and the methodology adopted [37–43].

Given this scenario, we look further at the isotropy of the Pantheon + SH0ES data. In this case, we carry out a directional analysis of the deceleration parameter (q_0) across the celestial sphere. Similar approaches were adopted in [40,43], although the authors focused on the H_0 and Ω_{m} parameters, as given by the standard model, i.e., within the flat ΛCDM framework. Instead, we rely on a cosmographic description of the Universe so that no further assumptions on its dynamic content, e.g., the nature of dark matter and dark energy, are needed—as long as we restrict our analysis to the lower redshift threshold of the sample. We also estimate the statistical significance of our results in

[*]carlosbengaly@on.br
[†]alcaniz@on.br
[‡]cpigozzo@ufba.br

light of the assumptions made on data analysis, or the non-uniformity of the SN sky distribution.

The paper is structured as follows: Sec. II is dedicated to explaining our method and the data selection and preparation. Section III presents the results obtained from this method, along with the statistical significance tests. Section IV provides the discussion and our concluding remarks.

II. METHOD

A. Data preparation

We use the Pantheon + SH0ES compilation, as retrieved from the Github repository.[1] This dataset consists on 1701 light curve measurements of 1550 distinct SNe within the $0.001 < z < 2.26$ redshift range, which also comprises 77 data points from Cepheid host galaxies at very low redshifts, i.e., $0.00122 < z < 0.01682$. Those measurements are designated in the data release as a Boolean variable, so that we use the Cepheid host distances provided in those cases, instead of the distance modulus measured by the corresponding SN. Note we use the redshift given in the zHD variable, since it includes the correction from the heliocentric to the cosmic microwave background rest-frame, as well as further corrections due to the nearby SN peculiar velocities [44,45]. Still, we caution that the effect of those peculiar velocities can lead to spurious anisotropy in the Hubble flow, if not properly accounted for [46–50]. Although some doubts have been cast on the modeling of the SN peculiar velocities in this sample (see Ref. [37]), we will not attempt to reevaluate their effects on the isotropy test we perform in this work.

It is important to avoid possible biases from the original sample as much as possible, because it consists of an SN compilation from observations performed by various surveys that have (or had) different designs and sky coverage. Thus, the original SN compilation is expected to be affected mainly by uneven sky coverage. Due to this, we impose two different redshift cutoffs before we proceed to the isotropy test. The first one consists of an upper redshift cutoff at the $z > 0.10$ range, since the SN sky distribution becomes much more sparse at higher redshifts (see upper panel of Fig. 1 for a visual explanation). This is something expected, since those objects were observed by spectroscopic surveys designed to cover only those specific regions of the sky, in order to obtain the highest-resolution spectroscopy possible. Also, we can safely use cosmographic expansion on Eq. (1) since it is a good approximation in that redshift range. Secondly, we impose a lower redshift cutoff at $z < 0.01$, except for the distance measurements within Cepheid host galaxies. Hence, we end up with a working sample of 697 SN data points, as displayed in the lower panel of Fig. 1.

[1] https://github.com/PantheonPlusSH0ES/DataRelease.

B. Estimator

We assume a cosmographic expression of the luminosity distance [51–53],

$$D_L(z) = (c/H_0)[z + (1 - q_0)z^2/2], \tag{1}$$

where H_0 and q_0 stand for the Hubble constant and the deceleration parameter, respectively, and $D_L(z)$ is given in Mpc. As the distance modulus definition reads

$$\mu_{\rm model}(z) \equiv m - M = 5\log_{10}(D_L(z)/\mathrm{Mpc}) + 25, \tag{2}$$

we obtain the best-fit for the q_0 through a χ^2 minimization, as given by

$$\chi^2 = \vec{\delta}^{\rm T}(C_{\rm stat+sys})^{-1}\vec{\delta}, \tag{3}$$

so that $C_{\rm stat+sys}$ denotes the full SN covariance matrix, and

$$\delta_{\rm i} = \begin{cases} m_{\rm i} - M - \mu_{\rm i}, & i \in \text{Cepheid hosts} \\ m_{\rm i} - M - \mu_{\rm model}(z_i) & \text{otherwise.} \end{cases} \tag{4}$$

We adopt the following estimator to test the isotropy of the local cosmic acceleration by a similar fashion of [40,43], as follows:

$$\Delta_{q0} = \frac{\left|q_0^{(\text{“northcap”})}\right| - \left|q_0^{(\text{“southcap”})}\right|}{\sigma^2_{q_0^{(\text{“northcap”})}} + \sigma^2_{q_0^{(\text{“southcap”})}}}, \tag{5}$$

where Δ_{q0} is given in units of confidence level (CL). We compute the best-fitted value for the deceleration parameters at opposite patches across the entire celestial sphere (60° size) along a specific axis randomly selected across the sky. A total of 500 axes were taken in our analysis. In Eq. (5), these quantities are denoted by $q_0^{(\text{“northcap”})}$, and $q_0^{(\text{“southcap”})}$, correspondingly, while $\sigma^2_{q_0^{(\text{“northcap”})}}$ and $\sigma^2_{q_0^{(\text{“southcap”})}}$ provides their respective uncertainties at 1σ CL. Explicitly, we do so by computing likelihoods of the $q_0^{(\text{“northcap”})}$, and $q_0^{(\text{“southcap”})}$ according to $\mathcal{L} \propto \exp -\chi^2/2$, where χ^2 corresponds to Eq. (3). Then, we use the CURVEFIT routine of the SciPy module to fit a Gaussian curve to the likelihoods at each cap, and we take its mean value and standard deviation as our corresponding q_0 and σ_{q_0} in each “north/south” cap, respectively, in Eq. (5).

Finally, we stress two more points: (i) We perform our analysis within 60° size spherical caps, instead of the typical choice of 90° size ones—which encompasses an entire hemisphere—for the sake of computational time. Nonetheless, we expect that this choice should not impact

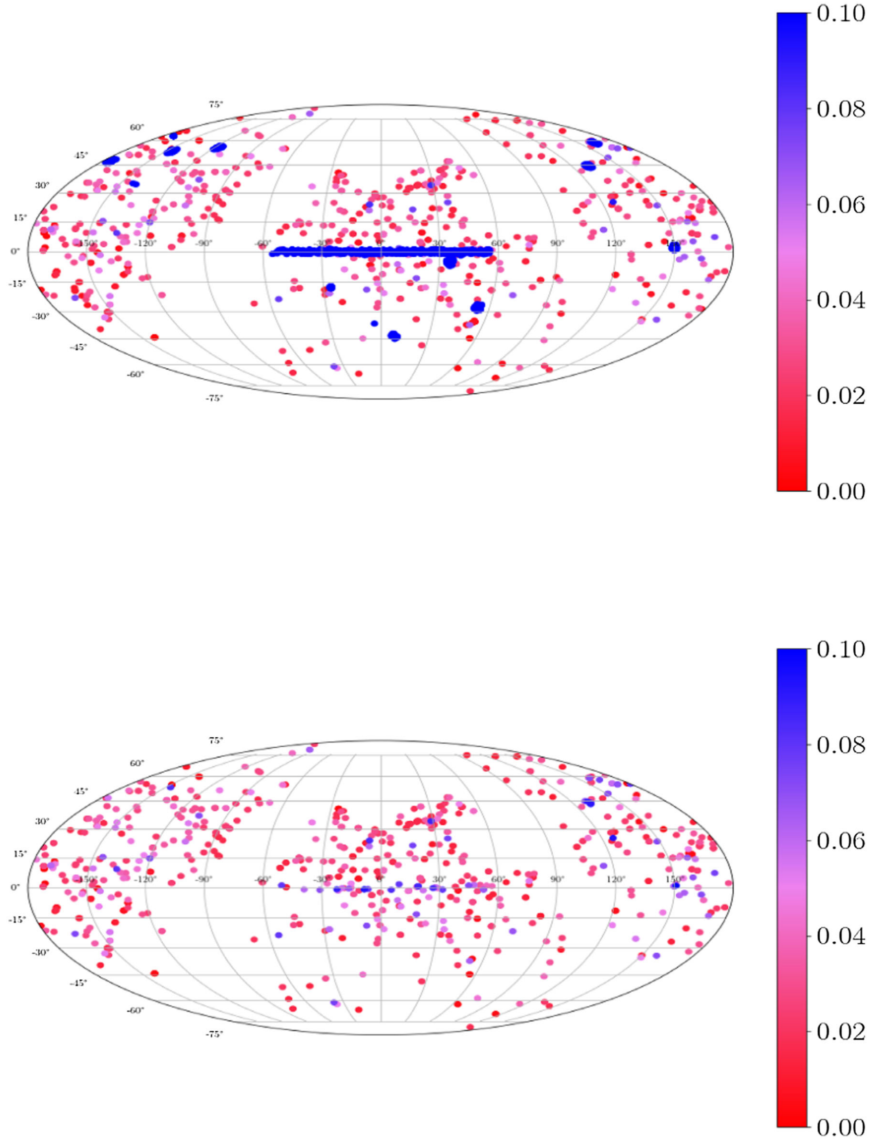

FIG. 1. A Mollweide projection of the SN positions in the sky. In the *upper panel*, we assign their positions in such a way that the color bar is truncated in $z = 0.1$, so that all SNe with $z > 0.1$ are shown in blue. On the other hand, the *lower panel* displays the SNe that made our imposed redshift cut, i.e., $0.01 < z < 0.10$, in addition to the SNe in Cepheid host galaxies, for a color range $z = 0$ (reddest) to $z = 0.1$ (bluest). Both maps are projected in celestial sky coordinates (RA, DEC).

our conclusions, as the results obtained from 60° caps show good agreement with those assuming 90° caps—see Fig. 18 in [43]; (ii) The fact that we are assuming a cosmographic expansion, rather than the exact expression for the luminosity distance in the ΛCDM framework, does not bias our inferences. The relative difference between the distance modulus predicted by both cases, assuming self-consistent cosmological parameters, i.e., $q_0 = -0.499$ for former, and $\Omega_m = 0.334$ for the latter—and both assuming $H_0 = 73.3\ \mathrm{km\,s^{-1}\,Mpc^{-1}}$—only differ at about 0.35% at $z = 0.1$, which is the highest redshift covered by our SN subsample. Since the uncertainties of the SN measurements are typically larger than those values, our analysis and conclusions should not be affected by that.

III. RESULTS

A. Real data analysis

We show the result of the Δ_{q0} analysis in the left panel of Fig. 2. We represent it as a map in Cartesian coordinates of the Δ_{q0} values obtained across the 500 randomly selected directions in the sky for the Pantheon + SH0ES SN sample. Here, Δ_{q0} is given in units of standard deviations. The green diamond mark displays the maximum anisotropy direction found, along the $(RA^{\rm SN}, DEC^{\rm SN}) = (267°, 6°)$ axis, as represented by the green dashed lines, while the black solid lines and black dotted mark represents the cosmic microwave background (CMB) dipole direction, i.e., $(RA^{\rm CMB}, DEC^{\rm CMB}) = (167°, -7°)$. We report a maximum Δ_{q0} value of $\Delta_{q0} = 3.06$ in this case.

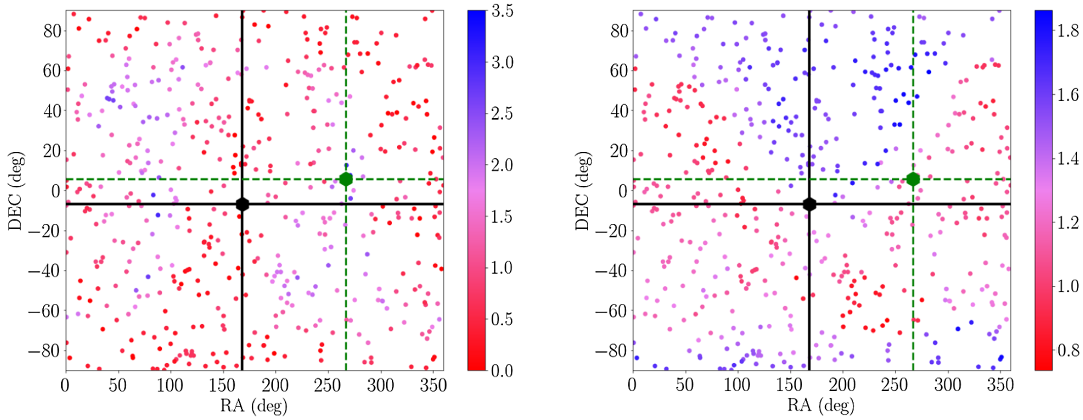

FIG. 2. *Left panel*: A Cartesian projection map of the Δ_{q0} analysis. We take 500 random directions on our Pantheon + SH0ES selected subsample, as represented by each coloured point in this map, for a color bar at the range $0 < \Delta_{q0} < 3.5$ (C.L.). The green diamond mark displays the maximum anisotropy direction, found along the $(RA^{\rm SN}, DEC^{\rm SN}) = (267°, 6°)$ axis, whereas the black dotted mark represents the axis of the CMB dipole direction, i.e., $(RA^{\rm CMB}, DEC^{\rm CMB}) = (167°, -7°)$. *Right panel*: Same as left panel, but rather for the reduced χ^2 value, $\chi^2_{\rm red}$, obtained in each of those random sky directions.

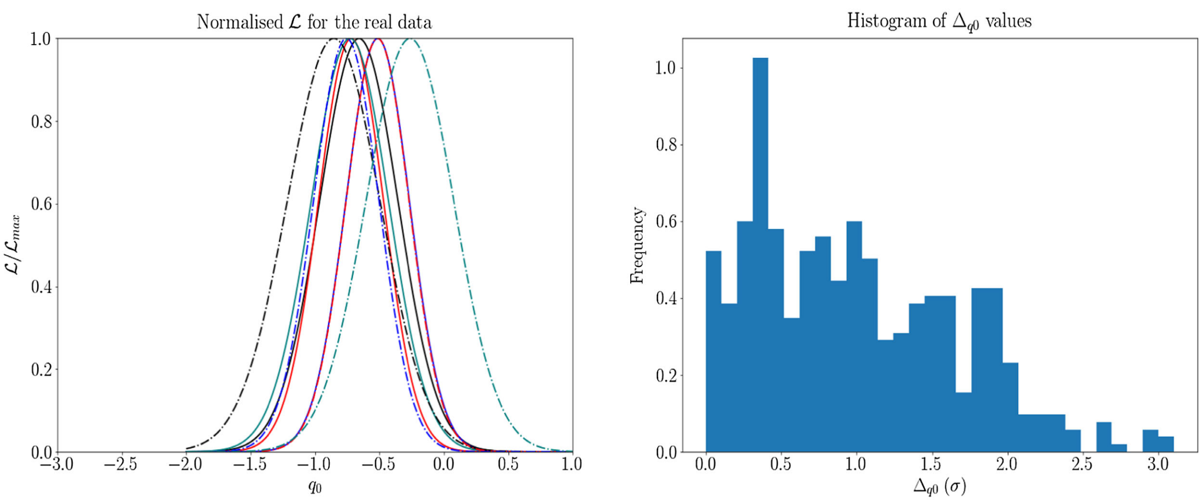

FIG. 3. *Left panel*: Examples of the q_0 normalized likelihood from four different directions across the sky. The black, red, blue and teal solid (dashed-dotted) curves represent the "northern" ("southern") counterpart of each of those directions. *Right panel*: A histogram of Δ_{q0} values, given in function of C.L. (σ).

For the sake of consistency, we also display the reduced χ^2 value in the right panel of the same figure, as defined by $\chi^2_{\rm red} \equiv \chi^2/{\rm d.o.f.}$, where d.o.f. denotes the number of degrees of freedom in each celestial cap, and χ^2 is given by Eq. (3). We can see that the bluest dots, which denote the poorest q_0 fits to the data, do not coincide with the bluest regions in the Δ_{q0} map. This result indicates that the largest Δ_{q0} values do not occur due to a poor fit of the data, and that the largest $\chi^2_{\rm red}$ values are rather due to undersampling of SN objects in the corresponding sky regions.

Accordingly, in the left panel of Fig. 3, we present examples of the normalized q_0 likelihood functions obtained from four different directions in the sky to visualize better the fits. In this case, different colors denote different sky directions, whereas the solid and dashed-dotted curves stand for the "northern" and "southern" counterpart of each direction respectively. In addition, the right panel of the same figure shows a histogram of the Δ_{q0} values, as given in confidence levels. We find that this distribution peaks at $\Delta_{q0} \sim 0.5$, which corresponds to the most frequent value for the q_0 anisotropy level, and that its maximum value is $\Delta_{q0} = 3.06$—as also shown in the left panel of Fig. 2.

B. Statistical significance of the results

As for the statistical significance of our results, we test three main cases: (i) How the Δ_{q0} values can be affected under the assumption of different H_0 values to be fixed in

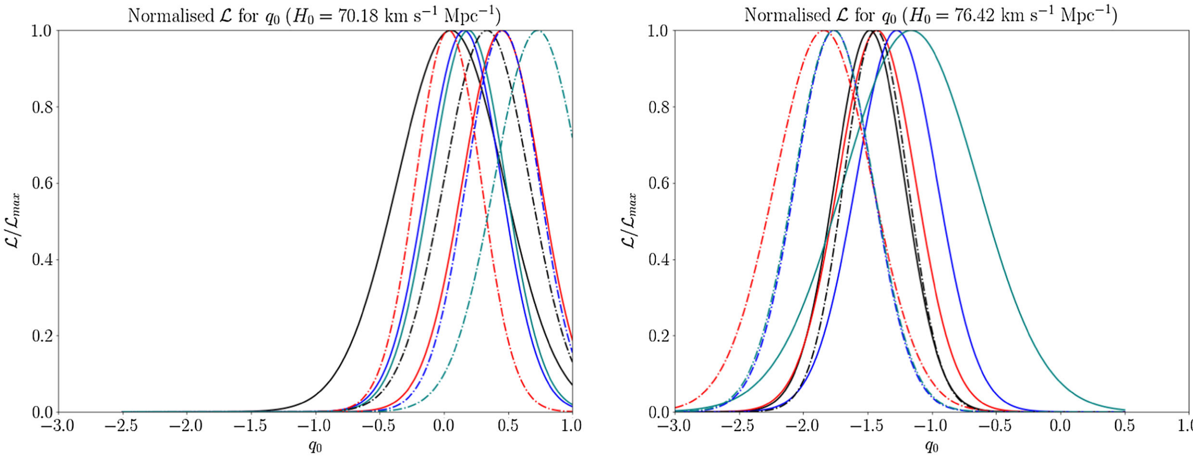

FIG. 4. Same as left panel of Fig. 3, but rather for the normalised likelihoods for q_0 when assuming different Hubble constant values, i.e., $H_0 = 70.18\ \mathrm{km\,s^{-1}\,Mpc^{-1}}$ (left panel), and $H_0 = 76.42\ \mathrm{km\,s^{-1}\,Mpc^{-1}}$ (right panel).

our analysis; (ii) How the Δ_{q0} values can be affected when assuming a fiducial q_0 value; (iii) How the Δ_{q0} values can be affected if the SN celestial distribution is considered uniform. In all three cases, we stress that we are assuming the same SN covariance matrix as the original one, apart from the redshift selection imposed.

As for case (i): In Fig. 4, we display the normalised likelihoods for q_0 when assuming different Hubble constant values, i.e., $H_0 = 70.18\ \mathrm{km\,s^{-1}\,Mpc^{-1}}$ (left panel), and $H_0 = 76.42\ \mathrm{km\,s^{-1}\,Mpc^{-1}}$ (right panel). We find that a higher H_0 value leads to highly negative values for the deceleration parameter. In contrast, the opposite trend occurs for lower H_0 values—see how those likelihoods are skewed to the right and left, respectively, compared to those shown in the left panel of Fig. 3, where we assumed the SH0ES H_0 measurement. Hence, we find that the q_0 fit is very sensitive to the H_0 assumption, which is an expected result, since this parameter is degenerated with the absolute magnitude M_B value—and so we would need to adjust M_B accordingly to the change in the H_0. We will leave a more thorough examination of the possible degeneracy in the (M_B, H_0, q_0) plane in a future work.

As for case (ii): In Fig. 5, we show the results obtained by means of a set of 200 realizations named *lcdm*. In this case, we fixed the observed modulus distance to the value given by the flat ΛCDM best-fit for q_0 from the original Pantheon + SH0ES, i.e., $q_0 = -0.499$, as $\Omega_{m0} = 0.334$ and thus $q_0 = (3/2)\Omega_{m0} - 1 = -0.499$. The goal is to assess the residuals of our q_0 best-fit estimator due to the limited sampling of SNe across the sky given our 60° patch size. As we can see in its left panel, we are able to robustly recover the fiducial q_0 best-fit in all cases, albeit with larger uncertainty in some of them—which naturally occur due to the SN sky sampling in those specific patches. On the other hand, the histogram displayed in the right panel shows a maximum value of $\Delta_{q0} = 0.24$ in those realizations. We interpret this result as the maximum variance we can expect from our analysis due only to the effect of the SN sample incompleteness across the celestial sphere.

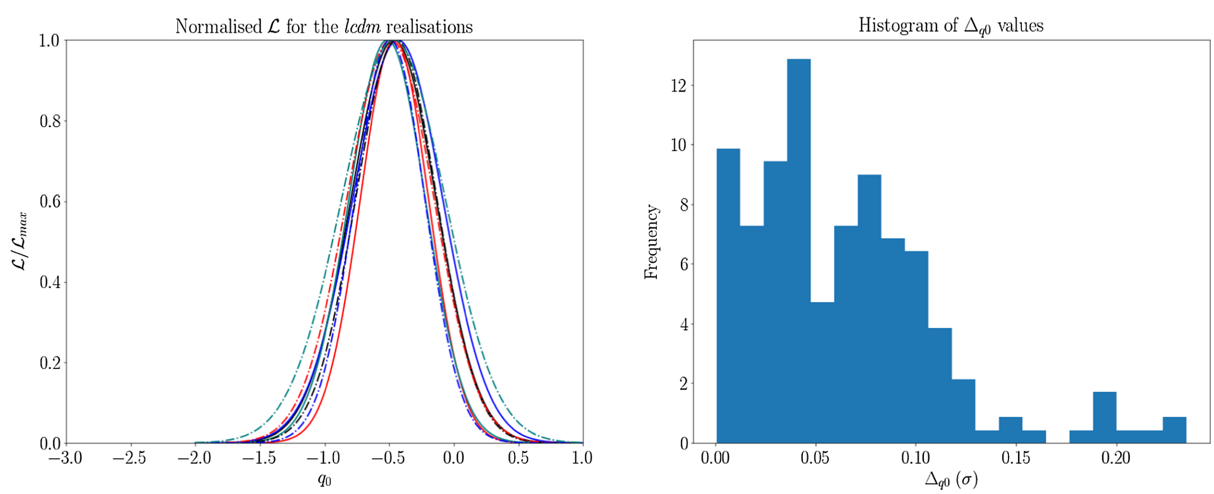

FIG. 5. Same as Fig. 3, but rather for the *lcdm* realizations.

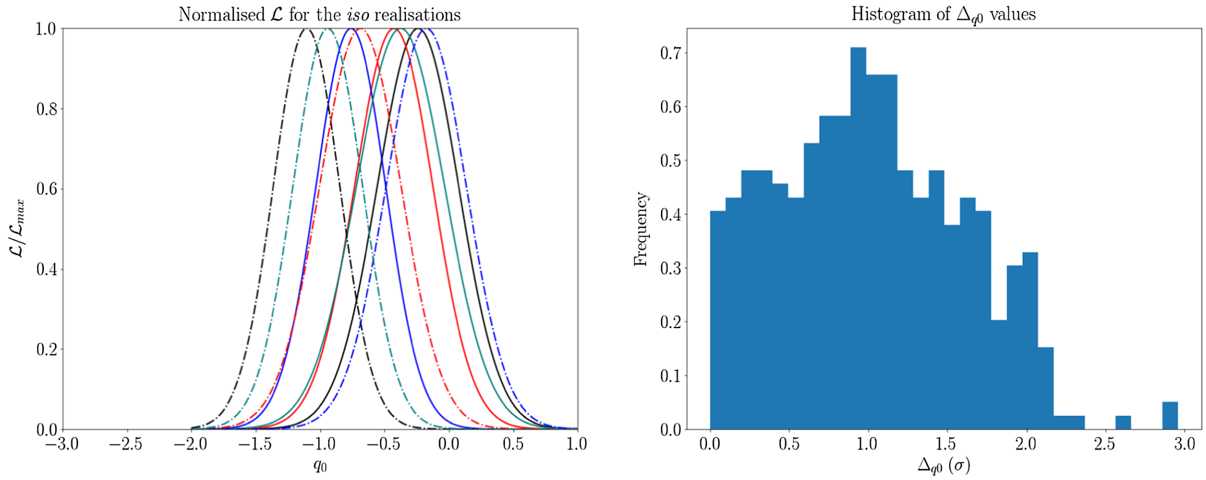

FIG. 6. Same as Fig. 5, but rather for the *iso* realizations.

As for case (iii): In Fig. 6, we present normalized q_0 for five realizations (left panel), and the Δ_{q0} histogram (right panel) for a set of 400 *iso* realizations. Conversely, from the previous cases, we assume a uniform SN sky distribution by replacing the original SN coordinates with a random direction across the celestial sphere. We obtain a maximum value of $\Delta_{q0} = 2.96$ in this case. Such a result is in good agreement with the $\Delta_{q0} = 3.06$ result obtained for the real data case—especially considering the $\Delta_{q0} = 0.24$ residual obtained for the *lcdm* realizations, as previously described. Therefore, we conclude that there is no statistically significant indication for a breakdown of the cosmic isotropy hypothesis in this case.

IV. DISCUSSION AND CONCLUSIONS

The validity of the cosmological principle, i.e., the large-scale isotropy and homogeneity of the Universe, constitutes one of the core assumptions of modern cosmology. Even though the available observational data favours the ΛCDM scenario based on this hypothesis, it has seldom been tested directly. Hence, developing and performing such tests is crucial since any hint of a statistically significant breakdown of such an assumption would require an extensive reformulation of the standard cosmological model from the basics.

We used the latest type Ia supernova compilation of distance measurements, namely the Pantheon + SH0ES data set to test the isotropy of the Universe. We did so by assessing the directional dependence of the deceleration parameter, where we split the data into subsets across randomly selected directions in the sky, in which we obtained their best-fitted values. After restricting our data to the $0.01 < z < 0.10$ range, except for the SN in Cepheid host galaxies, we found a maximum variation of $\Delta_{q0} = 3.06$ at roughly 90° from the CMB dipole direction—a signal ascribed to our relative motion concerning its rest frame. Moreover, we found that this result does not manifest from the assumptions made during the parameter estimation—e.g., by fixing the Hubble constant and SN absolute magnitude to its default values or by the incoherent fitting of the deceleration parameter—and most importantly, we found that such a variation is in good agreement with simulations assuming a uniform sky distribution of the SN data points. Therefore, we can conclude that this result is not statistically significant and that it should occur due to intrinsic fluctuations in the data—primarily due to the uncertainties in its covariance matrix.

Our results present an improvement from analyses made on the previous SN compilation, i.e., the Pantheon dataset, where it was found from similar tests that the directional dependence of the cosmological parameters could be ascribed to the inhomogeneous SN celestial distribution—see, for instance, [23]. In addition, we extend and complement former analyses in the literature [39–43], as we avoided the assumption of dark energy using the cosmographic expansion,[2] and performed more stringent cuts in the sample to avoid possible biases. Hence, in contrast with some of those results, we found no significant evidence for a possible deviation from the cosmological principle assumption in the Pantheon + SH0ES data. This is in good agreement with previous tests using other types cosmological observations, e.g. galaxy clusters [54], infrared galaxies [55], gamma ray bursts [56], and quasars [57].

Given the advent of ongoing and forthcoming redshift surveys, such as eROSITA [58], Vera C. Rubin Observatory [59], Euclid [60], Square Kilometer Array Observatory [61], besides distance measurements by standard sirens from LIGO and Einstein Telescope, we expect that this variance should be reduced even further, and thus, we will

[2]We note that future SN distance measurements might have to assume a higher order cosmographic expansion, as their respective uncertainties might get smaller than the 0.35% difference between the predictions from the cosmography expansion up to the second order in redshift, as assumed here, and the ΛCDM predictions.

be able to pinpoint if the cosmological principle provides a realistic representation of the Universe at large scales.

ACKNOWLEDGMENTS

C. B. acknowledges financial support from Fundação à Pesquisa do Estado do Rio de Janeiro (FAPERJ)—Postdoc Recente Nota 10 (PDR10) fellowship. J. S. A. is supported by CNPq Grant No. 307683/2022-2 and Fundação de Amparo à Pesquisa do Estado do Rio de Janeiro (FAPERJ) Grant No. 259610 (2021). This work was developed thanks to the National Observatory Data Center (CPDON).

[1] J. Goodman, Geocentrism reexamined, Phys. Rev. D **52**, 1821 (1995).
[2] C. Clarkson and R. Maartens, Inhomogeneity and the foundations of concordance cosmology, Classical Quantum Gravity **27**, 124008 (2010).
[3] R. Maartens, Is the Universe homogeneous?, Phil. Trans. R. Soc. A **369**, 5115 (2011).
[4] C. Clarkson, Establishing homogeneity of the universe in the shadow of dark energy, C.R. Phys. **13**, 682 (2012).
[5] P. K. Aluri, P. Cea, P. Chingangbam, M. C. Chu, R. G. Clowes, D. Hutsemékers, J. P. Kochappan, A. M. Lopez, L. Liu, N. C. M. Martens *et al.*, Is the observable Universe consistent with the cosmological principle?, Classical Quantum Gravity **40**, 094001 (2023).
[6] P. Laurent, J. M. Le Goff, E. Burtin, J. C. Hamilton, D. W. Hogg, A. Myers, P. Ntelis, I. Pâris, J. Rich, E. Aubourg *et al.*, A $14h^{-3}$ Gpc^3 study of cosmic homogeneity using BOSS DR12 quasar sample, J. Cosmol. Astropart. Phys. 11 (2016) 060.
[7] P. Ntelis, J. C. Hamilton, J. M. Le Goff, E. Burtin, P. Laurent, J. Rich, N. G. Busca, J. Tinker, E. Aubourg, H. Bourboux *et al.*, Exploring cosmic homogeneity with the BOSS DR12 galaxy sample, J. Cosmol. Astropart. Phys. 06 (2017) 019.
[8] R. S. Gonçalves, G. C. Carvalho, C. A. P. Bengaly, J. C. Carvalho, A. Bernui, J. S. Alcaniz, and R. Maartens, Cosmic homogeneity: A spectroscopic and model-independent measurement, Mon. Not. R. Astron. Soc. **475**, L20 (2018).
[9] R. S. Gonçalves, G. C. Carvalho, U. Andrade, C. A. P. Bengaly, J. C. Carvalho, and J. Alcaniz, Measuring the cosmic homogeneity scale with SDSS-IV DR16 quasars, J. Cosmol. Astropart. Phys. 03 (2021) 029.
[10] Y. Kim, C. G. Park, H. Noh, and J. c. Hwang, CMASS galaxy sample and the ontological status of the cosmological principle, Astron. Astrophys. **660**, A139 (2022).
[11] U. Andrade, R. S. Gonçalves, G. C. Carvalho, C. A. P. Bengaly, J. C. Carvalho, and J. Alcaniz, The angular scale of homogeneity with SDSS-IV DR16 luminous red galaxies, J. Cosmol. Astropart. Phys. 10 (2022) 088.
[12] T. S. Kolatt and O. Lahav, Constraints on cosmological anisotropy out to $z = 1$ from supernovae Ia, Mon. Not. R. Astron. Soc. **323**, 859 (2001).
[13] D. J. Schwarz and B. Weinhorst, (An)isotropy of the Hubble diagram: Comparing hemispheres, Astron. Astrophys. **474**, 717 (2007).
[14] I. Antoniou and L. Perivolaropoulos, Searching for a cosmological preferred axis: Union2 data analysis and comparison with other probes, J. Cosmol. Astropart. Phys. 12 (2010) 012.
[15] R. G. Cai and Z. L. Tuo, Direction dependence of the deceleration parameter, J. Cosmol. Astropart. Phys. 02 (2012) 004.
[16] B. Bahr-Kalus, D. J. Schwarz, M. Seikel, and A. Wiegand, Constraints on anisotropic cosmic expansion from supernovae, Astron. Astrophys. **553**, A56 (2013).
[17] W. Zhao, P. X. Wu, and Y. Zhang, Anisotropy of cosmic acceleration, Int. J. Mod. Phys. D **22**, 1350060 (2013).
[18] J. Beltran Jimenez, V. Salzano, and R. Lazkoz, Anisotropic expansion and SNIa: An open issue, Phys. Lett. B **741**, 168 (2015).
[19] Z. Chang, X. Li, H. N. Lin, and S. Wang, Constraining anisotropy of the universe from different groups of Type-Ia supernovae, Eur. Phys. J. C **74**, 2821 (2014).
[20] C. A. P. Bengaly, A. Bernui, and J. S. Alcaniz, Probing cosmological isotropy with Type IA supernovae, Astrophys. J. **808**, 39 (2015).
[21] B. Javanmardi, C. Porciani, P. Kroupa, and J. Pflamm-Altenburg, Probing the isotropy of cosmic acceleration traced by Type Ia supernovae, Astrophys. J. **810**, 47 (2015).
[22] H. K. Deng and H. Wei, Null signal for the cosmic anisotropy in the Pantheon supernovae data, Eur. Phys. J. C **78**, 755 (2018).
[23] U. Andrade, C. A. P. Bengaly, B. Santos, and J. S. Alcaniz, A model-independent test of cosmic isotropy with low-z pantheon supernovae, Astrophys. J. **865**, 119 (2018).
[24] J. Colin, R. Mohayaee, M. Rameez, and S. Sarkar, Evidence for anisotropy of cosmic acceleration, Astron. Astrophys. **631**, L13 (2019).
[25] D. Zhao, Y. Zhou, and Z. Chang, Anisotropy of the Universe via the Pantheon supernovae sample revisited, Mon. Not. R. Astron. Soc. **486**, 5679 (2019).
[26] L. Kazantzidis and L. Perivolaropoulos, Hints of a local matter underdensity or modified gravity in the low z Pantheon data, Phys. Rev. D **102**, 023520 (2020).
[27] J. P. Hu, Y. Y. Wang, and F. Y. Wang, Testing cosmic anisotropy with Pantheon sample and quasars at high redshifts, Astron. Astrophys. **643**, A93 (2020).
[28] A. Salehi, H. Farajollahi, M. Motahari, P. Pashamokhtari, M. Yarahmadi, and S. Fathi, Are Type Ia supernova powerful tool to detect anisotropic expansion of the Universe?, Eur. Phys. J. C **80**, 753 (2020).
[29] D. Zhao and J. Q. Xia, A tomographic test of cosmic anisotropy with the recently-released quasar sample, Eur. Phys. J. C **81**, 948 (2021).

[30] C. Krishnan, R. Mohayaee, E. Ó. Colgáin, M. M. Sheikh-Jabbari, and L. Yin, Hints of FLRW breakdown from supernovae, Phys. Rev. D **105**, 063514 (2022).
[31] W. Rahman, R. Trotta, S. S. Boruah, M. J. Hudson, and D. A. van Dyk, New constraints on anisotropic expansion from supernovae Type Ia, Mon. Not. R. Astron. Soc. **514**, 139 (2022).
[32] N. Horstmann, Y. Pietschke, and D. J. Schwarz, Inference of the cosmic rest-frame from supernovae Ia, Astron. Astrophys. **668**, A34 (2022).
[33] S. Dhawan, A. Borderies, H. J. Macpherson, and A. Heinesen, The quadrupole in the local Hubble parameter: First constraints using Type Ia supernova data and forecasts for future surveys, Mon. Not. R. Astron. Soc. **519**, 4841 (2023).
[34] D. Brout, D. Scolnic, B. Popovic, A. G. Riess, J. Zuntz, R. Kessler, A. Carr, T. M. Davis, S. Hinton, D. Jones *et al.*, The Pantheon+ analysis: Cosmological constraints, Astrophys. J. **938**, 110 (2022).
[35] D. Scolnic, D. Brout, A. Carr, A. G. Riess, T. M. Davis, A. Dwomoh, D. O. Jones, N. Ali, P. Charvu, R. Chen *et al.*, The Pantheon+ analysis: The full data set and light-curve release, Astrophys. J. **938**, 113 (2022).
[36] A. G. Riess, W. Yuan, L. M. Macri, D. Scolnic, D. Brout, S. Casertano, D. O. Jones, Y. Murakami, L. Breuval, T. G. Brink *et al.*, A comprehensive measurement of the local value of the Hubble constant with 1 $\mathrm{km\,s^{-1}\,Mpc^{-1}}$ uncertainty from the Hubble space telescope and the SH0ES Team, Astrophys. J. Lett. **934**, L7 (2022).
[37] F. Sorrenti, R. Durrer, and M. Kunz, The dipole of the Pantheon + SH0ES data, J. Cosmol. Astropart. Phys. 11 (2023) 054.
[38] J. A. Cowell, S. Dhawan, and H. J. Macpherson, Potential signature of a quadrupolar Hubble expansion in Pantheon + supernovae, Mon. Not. R. Astron. Soc. **526**, 1482 (2023).
[39] E. Pastén and V. H. Cárdenas, Testing ΛCDM cosmology in a binned universe: Anomalies in the deceleration parameter, Phys. Dark Universe **40**, 101224 (2023).
[40] R. Mc Conville and E. Ó. Colgáin, Anisotropic distance ladder in Pantheon + supernovae, Phys. Rev. D **108**, 123533 (2023).
[41] L. Perivolaropoulos, Isotropy properties of the absolute luminosity magnitudes of SnIa in the Pantheon+ and SH0ES samples, Phys. Rev. D **108**, 063509 (2023).
[42] L. Tang, H. N. Lin, L. Liu, and X. Li, Consistency of Pantheon + supernovae with a large-scale isotropic universe, Chin. Phys. C **47**, 125101 (2023).
[43] J. P. Hu, Y. Y. Wang, J. Hu, and F. Y. Wang, Testing the cosmological principle with the Pantheon+ sample and the region-fitting method, Astron. Astrophys. **681**, A88 (2024).
[44] E. R. Peterson, W. D'Arcy Kenworthy, D. Scolnic, A. G. Riess, D. Brout, A. Carr, H. Courtois, T. Davis, A. Dwomoh, D. O. Jones *et al.*, The Pantheon+ analysis: Evaluating peculiar velocity corrections in cosmological analyses with nearby Type Ia supernovae, Astrophys. J. **938**, 112 (2022).
[45] A. Carr, T. M. Davis, D. Scolnic, D. Scolnic, K. Said, D. Brout, E. R. Peterson, and R. Kessler, The Pantheon+ analysis: Improving the redshifts and peculiar velocities of Type Ia supernovae used in cosmological analyses, Pub. Astron. Soc. Aust. **39**, e046 (2022).
[46] W. A. Hellwing, A. Nusser, M. Feix, and M. Bilicki, Not a copernican observer: Biased peculiar velocity statistics in the local Universe, Mon. Not. R. Astron. Soc. **467**, 2787 (2017).
[47] C. A. P. Bengaly, J. Larena, and R. Maartens, Is the local Hubble flow consistent with concordance cosmology?, J. Cosmol. Astropart. Phys. 03 (2019) 001.
[48] B. Kalbouneh, C. Marinoni, and J. Bel, Multipole expansion of the local expansion rate, Phys. Rev. D **107**, 023507 (2023).
[49] R. Maartens, J. Santiago, C. Clarkson, B. Kalbouneh, and C. Marinoni, Covariant cosmography: The observer-dependence of the Hubble parameter, arXiv:2312.09875.
[50] B. Kalbouneh, C. Marinoni, and R. Maartens, Cosmography of the local Universe by multipole analysis of the expansion rate fluctuation field, arXiv:2401.12291.
[51] S. Weinberg, *Gravitation and Cosmology: Principles and Applications of the General Theory of Relativity* (John Wiley and Sons, New York, 1972), ISBN 978-0-471-92567-5, 978-0-471-92567-5.
[52] M. Visser, Jerk and the cosmological equation of state, Classical Quantum Gravity **21**, 2603 (2004).
[53] C. Cattoen and M. Visser, Cosmography: Extracting the Hubble series from the supernova data, arXiv:gr-qc/0703122.
[54] C. A. P. Bengaly, A. Bernui, J. S. Alcaniz, and I. S. Ferreira, Probing cosmological isotropy with Planck Sunyaev–Zeldovich galaxy clusters, Mon. Not. R. Astron. Soc. **466**, 2799 (2017).
[55] C. A. P. Bengaly, C. P. Novaes, H. S. Xavier, M. Bilicki, A. Bernui, and J. S. Alcaniz, The dipole anisotropy of WISE × SuperCOSMOS number counts, Mon. Not. R. Astron. Soc. **475**, L106 (2018).
[56] U. Andrade, C. A. P. Bengaly, J. S. Alcaniz, and S. Capozziello, Revisiting the statistical isotropy of GRB sky distribution, Mon. Not. R. Astron. Soc. **490**, 4481 (2019).
[57] V. Mittal, O. T. Oayda, and G. F. Lewis, The cosmic dipole in the quaia sample of quasars: A Bayesian analysis, Mon. Not. R. Astron. Soc. **527**, 8497 (2024).
[58] A. Merloni, G. Lamer, T. Liu, M. E. Ramos-Ceja, H. Brunner, E. Bulbul, K. Dennerl, V. Doroshenko, M. J. Freyberg, S. Friedrich *et al.*, The SRG/eROSITA all-sky survey: First x-ray catalogues and data release of the western Galactic hemisphere, Astron. Astrophys. **682**, A34 (2024).
[59] P. A. Abell *et al.* (LSST Science and LSST Project Collaborations), LSST Science Book, Version 2.0, arXiv:0912.0201.
[60] L. Amendola, S. Appleby, A. Avgoustidis, D. Bacon, T. Baker, M. Baldi, N. Bartolo, A. Blanchard, C. Bonvin, S. Borgani *et al.*, Cosmology and fundamental physics with the Euclid satellite, Living Rev. Relativity **21**, 2 (2018).
[61] D. J. Bacon *et al.* (SKA Collaboration), Cosmology with Phase 1 of the Square Kilometre Array: Red Book 2018: Technical specifications and performance forecasts, Pub. Astron. Soc. Aust. **37**, e007 (2020).